

# WITHDRAWN: A Bias Gantry Profiling Boom Sprayer for Orchard Protection

Peng Huo

Hebei Agricultural University <https://orcid.org/0000-0002-0316-7872>

Jianping Li

[ljpnd327@126.com](mailto:ljpnd327@126.com)

Hebei Agricultural University <https://orcid.org/0000-0003-2807-3888>

---

## Research Article

**Keywords:** Dwarf rootstock and densely planted, Apple orchard, Profiling, Precision application.

**Posted Date:** June 14th, 2021

**DOI:** <https://doi.org/10.21203/rs.3.rs-593797/v1>

**License:**   This work is licensed under a Creative Commons Attribution 4.0 International License.

[Read Full License](#)

**Additional Declarations:** No competing interests reported.

---

## EDITORIAL NOTE:

The full text of this preprint has been withdrawn, as it was submitted in error. Therefore, the authors do not wish this work to be cited as a reference. Questions should be directed to the corresponding author.

# Abstract

An air-assisted sprayer sends liquid medicine to a canopy of orchard plants for protection. However, the inherent drift in this method lowers the pesticide utilization. To meet the gardening requirements of a short-anvil densely planted apple orchard, a profiling boom sprayer was designed, and the operation requirements and prototype operation parameters of plant protection were determined. The droplet depositions in the upper, middle, and lower layers of the targets and in the inner, middle and outer rings were analyzed in field experiments. The standard deviations of the droplet deposition coverage rates on free, slender, and high spindles at different heights were 4.43, 2.82, and 5.29, respectively, and those of the droplet deposition densities were 5.97, 4.98, and 6.15, respectively. All p-values exceeded 0.05, indicating that droplets from the outer ring were uniformly distributed at different canopy heights. The average droplet deposition density exceeded  $150 \text{ grains}\cdot\text{cm}^{-2}$  in the outer and center rings of the three tree-shaped targets, and reached  $100.60 \text{ grains}\cdot\text{cm}^{-2}$  in the inner ring. The droplet deposition coverage rates on the free, slender, and high spindles in the inner ring were 37.41%, 36.69%, and 35.47%, respectively, indicating that the droplet penetration ability of the profiling boom sprayer meets the requirements of plant protection. The developed profiling boom sprayer has improved the inherent serious drift problem of the air blower sprayer, and has provided inspiration for the research and development of orchard plant protection machinery.

**Materials and Methods:** water-sensitive paper produced by Liuliu Shanxia Plant Protection Technology Co., Ltd. (China); the profiling boom sprayer; a tractor; a wind-speed measuring instrument (AS856S, Shanghai Xima Technology (Group) Co., Ltd., Shanghai, China); a temperature and humidity measuring instrument (RC-4, Jiangsu Jingchuang Electric Co., Ltd., Jiangsu, China);, double-sided tape; a box ruler; a stopwatch and a scanner.

The water-sensitive paper was cut into  $3 \text{ cm} \times 2 \text{ cm}$  rectangular units, and its back side was pasted to the apple trees of the test target with a small amount of double-sided tape. Facing the east, south, west, and north directions, papers sprayed by the inner, middle and outer rings were pasted on the top, middle and bottom layers of the fruit tree canopy (Dong et al., 2018, Fig.5a). To avoid disturbance from spray drift, six fruit trees were selected as the test targets at intervals of their tree shapes, and 648 water-sensitive papers in total were pasted.

**Results:** After averaging over height, the standard deviations of the droplet deposition coverage rates of the free, slender, and high spindles were 4.43, 2.82, and 5.29 respectively, and those of the droplet deposition density were 5.97, 4.98, and 6.15 respectively. All p-values exceeded 0.05. The average droplet deposition densities of the three tree-shaped targets exceeded  $150 \text{ grains}\cdot\text{cm}^{-2}$  in the center and outer rings. The average droplet deposition density in the inner ring was  $100.60 \text{ grains}\cdot\text{cm}^{-2}$ , and the droplet deposition coverage rates of the free, slender, and high spindles were 37.41%, 36.69%, and 35.47%, respectively. Averaged over the four directions, the coverage rate in the outer ring was 41.46% higher than in the center ring, and 90.87% higher than in the inner ring. Meanwhile, the average coverage rate was 34.93% higher in the center ring than in the inner ring.

**Discussion:** The outer ring of the profiling boom sprayer evenly distributed the droplets at different heights. The growths of the droplet deposition coverage rates were similar, and the droplet penetrations in different rings were consistent. Although the droplet penetration of the inner ring was poorer in the horizontal than center and outer ring in the vertical direction, the blades of the inner ring were sprayed sufficiently to meet both the quality assessment of plant protection operations and the design operating requirements of the profiling boom sprayer.

## Introduction

The constant development and renewal of machinery for orchard plant protection has led to profile-modeled pesticide application technologies (Bahlol et al., 2020; Duga et al., 2015; Kira et al., 2018; Lin et al., 2020; Nan et al., 2019).

Profiling applications have been realized through canopy recognition technology (Salcedo et al., 2020; Berk et al., 2020; Hołownicki et al., 2017; Sinh et al., 2020; Torrent et al., 2020). Various researchers have attempted position and attitude control of the sprinkler head (Ma. et al., 2020; Herbst. et al., 2018; Balsari. et al., 2017; Mawer. et al., 1989; Ma. et al., 2019). New profiling sprayers were developed by Peteinatos et al. (2019) and Duga et al. (2017). On a canopy of fruit trees, Landers et al. (2010) showed that an adjustable air guide plate increases the deposition by up to 30%, and reduces the drift by 75%. Based on commercial winded sprayers with centrifuges and hydraulic nozzles, Baldoin et al. (2008) developed a liquid medicine reclaimable sprayer that wraps a canopy of grape vines. The excess liquid medicine is collected by vertical panels set on both sides of the fruit tree, rescuing 32% of the liquid medicine.

The first problem is uneven application at different heights. Modelers imitate different fruit trees, which have different planting patterns, and most models are limited to the local characteristics of fruit trees. In fact, the geographical conditions vary in different parts of the world, and profile spray machines often cannot reach the heights of spindle-shaped orchards. Therefore, a profile sprayer that adjusts to different heights and canopy widths is required.

The second problem is application distance, which varies the application amount. Air-assisted spraying has shaped the existing spraying technology because it delivers fine droplets that strongly penetrate the air. However, the fan is a fixed installation that cannot evenly access different parts of the canopy. Therefore, a profiled spray machine should closely approach the canopy and apply a uniform spray to all canopy parts.

Boom sprayers have not been considered in orchard plant protection. In profile-modeling spray technology, the profile-modeling variables of nozzle flow rate and fan-air flow rate usually assume an air-assisted sprayer as the carrier (Li et al., 2017). In the popular planting pattern of modern standardized apple orchards, the fruit trees are almost identically shaped. Applying a spray-rod sprayer might avoid the serious drift problem of the air-blast sprayer from the source, thereby realizing the goal of plant protection with reduced drug use.

To resolve the difficulty of profile-modeling spraying at different application heights and distances in apple orchards and the drift problem of the air-assisted sprayer, the present study designs a profile spray-rod sprayer that adapts to different tree shapes, heights, and canopy widths.

## **Horticultural Characteristics**

### **Cultivation mode of apple tree**

To avoid the contradiction between crown size and nutrient area, many apple orchardists adopt the close-planting pattern of wide-row dwarf rootstock. Wang et al. (2019) developed the “Sanyou” apple dwarf rootstock planting mode with fine varieties, fine rootstocks, and fine methods that fully comply with the ecological conditions. In the present study, the apple tree parameters were sampled at Lvyang Modern Agricultural Park (38° N, 114° E), located in the middle and north parts of Hebei Province, China (Fig. 1). Dwarf apple trees are early flowerers and fruiters, produce high yields of good quality fruit with high efficiency, and are well ventilated with good light transmission. Moreover, owing to their small size, they are easy to manage, labor-saving, and amenable to standardized and mechanized management.

### **Tree features**

Wide-row and narrow-row spacing cultivation of apple trees is favored for mechanized operation. As the trees are well ventilated and exposed to high light-transmission conditions, the fruits are high-quality with good coloring. The row spacing is comprehensively determined according to the fertilizer used, water conditions, varieties planted, and management level. At the study site, 80–160 plants cover an area of 667 m<sup>2</sup>: 83 plants at a spacing of 4 m × 2 m, and 111 plants at a spacing of 4 m × 1.5 m. To form wide rows with narrow spacing, the plants are arranged in a “wall” structure, which facilitates mechanization and assembly line operations. At present, most fruit farmers select a spindle-shaped tree structure for their apple orchards, which reduces the management, labor, and time costs (Jamar et al., 2010). The intermediate stock is dwarfing stock SH40. The tree body is fixed by wire through a five-line system to ensure its vertical growth, non-lodging, non-breaking, neat tree shape, and a smooth mechanical working road between rows. In terms of shape, spindles are divided into free, slender, and high spindles (Fig. 2). Spindles are characterized as follows: crown size 1.0–1.5 m, tree height 2.5–3.5 m, many side branches (free spindle); crown size 0.8–1.2 m, tree height 3.0–3.5 m, at least 15–20 side branches on the trunk (slender spindle); crown size 0.8–1.2 m, tree height 3.5–4.0 m, 20–30 lateral branches (high spindle).

### **Technical requirements for plant protection**

To administer the drug, chemical agents dissolved in water or oil, suspensions of wettable powders, oils, or mixed emulsions of oil and water were sprayed and dispersed into small droplets, and then uniformly distributed on the surfaces of the control object. In traditional pesticide spraying technology, the precision of spraying distance between the spray head and the target tree is low, and the droplets are unevenly distributed over different areas of the tree canopy. Profile spray modeling is a new technology for pesticide spraying on fruit trees, and has developed along with modern fine agriculture. The technology

detects the actual shape of fruit trees and controls the spray head at the ideal spraying distance, thereby improving the uniformity of droplet distribution on the fruit trees (Garcerá et al., 2020).

The present research aims to design a spray-rod deformation mechanism that adjusts the height of the spray rod and the distance between the spray rod and canopy to different tree shapes. Even in a standard orchard, there are non-ideal conditions such as indefinite row spacing, uneven height differences among the same kinds of fruit trees, and different crown shapes and densities. Therefore, the mechanical system should adjust the spatial position and posture of the sprinkler head in both the horizontal and vertical directions. Maintaining a proper distance of the sprinkler head from the tree crown can achieve profile modeling with low-volume spraying.

The overall design must consider the overall performance and structure of the device, which depends on the use of the device and the manufacturing and working conditions. The proposed technical requirements are listed below:

- (1) The spray rod can apply the medicine to the outer edge of the fruit tree-shaped enveloping canopy.
- (2) The spraying device can advance steadily through the field without failure or overturning.
- (3) In orchard protection, the droplet deposition coverage rate is at least 33%.
- (4) In orchard protection, the droplet deposition density exceeds  $70 \text{ grains}\cdot\text{cm}^{-2}$ .
- (5) The upper, middle, and lower parts of the canopy are evenly distributed, and the inner, center, and outer rings penetrations are good.

## Design Of The Profiling Boom Sprayer

### *Principle of mimetic application*

The spray-rod application covers the outer canopy edge of the free-spindle, slender-spindle, and high-spindle apple trees in the modern dwarf rootstock orchard, thus reducing the liquid loss by a certain extent. The operating principle of the profile-mimicking pesticide application is shown in Fig. 3, and the key structural parameters of the application are listed in Table 1.

### *Structure of the device*

When designing the overall structure of the profiling boom sprayer, we must consider the operating conditions of the sprayer, the performance stability, the characteristics of the operation, and the convenience of installation in the field. The spraying device must also operate reliably, and requires appropriate supporting equipment. The structure is compact, the mechanism connection and working parts are sufficiently strong and rigid, and the movement of the part assembly is smooth.

The profiling boom sprayer is mainly composed of the boom group, a medicine tank, a chassis, a diaphragm pump, a hydraulic station distributor, a solenoid valve group, a lifting mechanism, and a folding–unfolding mechanism (Fig. 4). The most basic component is the chassis, which carries the lifting mechanism, folding–unfolding mechanism, boom group, medicine tank, and hydraulic station distributor. The chassis is connected to a tractor through its front triangular structure to realize traction. It is equipped with a suspension that dampens the device when driving through the orchard, guaranteeing the stability of the pesticide application device. The lifting mechanism, which consists of a slide rail and a hydraulic cylinder, is welded to the chassis and is driven by the hydraulic cylinder. The folding–unfolding mechanism consists of a double parallel four-bar mechanism and is driven by another hydraulic cylinder. The hydraulic station provides two oil circuits, which respectively supply oil to the hydraulic cylinders of the lifting and folding–unfolding mechanisms. The diaphragm pump expels the liquid medicine from the medicine tank and delivers it to the boom group through the solenoid valve group connected to the spray rods of each level of the boom group. The solenoid valves control the switch of each nozzle and adjust the spray volume.

The boom group is the main working part of the profiling boom sprayer. The large size of the boom and the inconvenient transportation and storage processes (Gil. et al., 2014) necessitate a multi-stage boom design. The boom group in this research is divided into five stages and consists of spray booms that complete the work through folding, unfolding, and telescopic actions.

The lifting mechanism is composed of three-stage slide rails. The signal is transmitted to the central processing unit (CPU) through an ultrasonic sensor on the boom group. The CPU processes and issues control commands. The three-stage hydraulic cylinder drives the vertical motion of the lifting mechanism, and the folding–unfolding mechanism then adjusts the boom group to the spray working height.

## **Field Test Of The Profiled Boom Sprayer**

### *Test plan*

The field test was conducted in Lvyang Modern Agricultural Park (38° N, 114° E), Hebei Province, China, on August 30 of 2020. The average temperature and humidity in the test environment were 36.3°C and 54%, respectively. The average natural wind speed was 0.315 m/s. The experimental subjects were Fuji apple trees with 5-year-old dwarf rootstock planted in the north–south direction. The spray qualities were measured on free, slender, and high spindles, and fog droplets were detected on water-sensitive paper produced by Liuliu Shanxia Plant Protection Technology Co., Ltd. (China).

The main test instruments were the profiling boom sprayer supported on a tractor, a wind-speed measuring instrument (AS856S, Shanghai Xima Technology (Group) Co., Ltd., Shanghai, China), a temperature and humidity measuring instrument (RC-4, Jiangsu Jingchuang Electric Co., Ltd., Jiangsu, China), water-sensitive paper, double-sided tape, a box ruler, a stopwatch, and a scanner. The water-sensitive paper was cut into 3 cm × 2 cm rectangular units, and its back side was pasted to the apple trees of the test target with a small amount of double-sided tape. Facing the east, south, west, and north

directions, papers sprayed by the inner, middle and outer rings were pasted on the top, middle and bottom layers of the fruit tree canopy (Dong et al., 2018, Fig.5). To avoid disturbance from spray drift, six fruit trees were selected as the test targets at intervals of their tree shapes, and 648 water-sensitive papers in total were pasted.

After starting the tractor, the parameters of the profile-spray-bar sprayer were adjusted to the optimal spray conditions. The spray nozzle adopted an ARAG imported from Italy with a spray angle of  $110^\circ$ . The sprayers were separated by 0.39 m and their pressure was 0.74 MPa, giving a spray distance of 1.49 m. The tractor was operated at  $3.6 \text{ km}\cdot\text{h}^{-1}$ .

The water-sensitive papers were detached from the trees and pasted onto A4-sized paper sheets. As an example, Fig. 6 shows the water-sensitive paper from one of the test targets.

To collect the fog drop information, the water-sensitive papers were scanned using Image-master software. The sigma and weight parameters were both set to 5, and the analysis area was selected and extracted. After adjusting the foreground and background pixels in the area, the foreground background stripping, foreground removal, and noise-reduction processing were adjusted using the "threshold adjustment" functionality. Finally, the total number of droplets, droplet deposition coverage rates, and droplet deposition densities were derived from the processed water-sensitive paper (see Fig. 7).

### *Analysis of test results*

The test results were analyzed in terms of spraying quality of the plant protection equipment. For convenience, the top, middle and bottom layers are represented by T, M, and B, respectively, the east, west, south, and north directions are represented by E, W, S, and N, respectively, and the inner, center, and outer rings are represented by I, C, and O, respectively. To analyze the droplet distribution in the outer ring of the target, the droplet deposition coverage rates from that ring were counted at different heights (Fig. 8).

The droplet deposition coverage rates were subjected to single-factor analysis of variance (ANOVA) and the results are shown in Table 2. All p-values were greater than 0.05, indicating no significant differences in the droplet deposition coverage rates at different heights in different directions. The standard deviations of the droplet deposition coverage rates of the outer rings on the free, slender, and high spindles at different heights were 4.43, 2.82, and 5.29, respectively, indicating small variations in the droplet deposition coverage rates for a particular tree shape. Clearly, the outer-ring droplets expelled from the profiling boom sprayer were evenly distributed over the height of the test target.

The droplet deposition densities on the target of the outer ring were counted at different heights, and the results are presented in Fig. 9. From these results, the effect of the medicine application on the leaves of the outer-ring target was analyzed.

Table 3 lists the deposition densities on the targets of the outer ring, obtained by single-factor ANOVA. All p-values exceeded 0.05, indicating no significant difference in the droplet deposition densities at different

heights in any direction. The standard deviations of the droplet deposition densities of the free, slender, and high spindles from the outer rings at different heights were 5.97, 4.98, and 6.15, respectively, indicating small differences in the deposition densities on a particular tree shape. Clearly, the outer-ring blades of the profiling boom sprayer uniformly coated the test target.

Figure 10 shows the droplet deposition coverage rates on the targets of the inner, center, and outer rings in different directions. From these results, the distribution characteristics of the inner, center, and outer rings were analyzed. In any given region, the droplet deposition coverage rates in each direction were similar to those of the outer ring; specifically, the average coverage was higher in the E and W directions (charging side) than in the S and N directions (non-charging side). Averaged over the three tree shapes, the droplet deposition coverage rates of the inner, center, and outer rings were 2.59%, 4.63%, and 7.50% respectively.

The droplet deposition coverage rate suddenly increased between the inner and outer rings. Averaged over the four directions, the coverage rate in the outer ring was 41.46% higher than in the center ring, and 90.87% higher than in the inner ring. Meanwhile, the average coverage rate was 34.93% higher in the center ring than in the inner ring, indicating that fog reached the outer and center rings. The growths of the droplet deposition coverage rates were similar, and the droplet penetrations in different rings were consistent. The average droplet deposition coverage rates of the inner rings of the free, slender, and high spindles were 37.41%, 36.69% and 35.47%, respectively, lower than in the outer rings but still exceeding 33%. Although the droplet penetration of the inner ring was poorer in the horizontal than center and outer ring in the vertical direction, the blades of the inner ring were sprayed sufficiently to meet both the quality assessment of plant protection operations and the design operating requirements of the profiling boom sprayer (NY/T 992-2006).

The deposition densities on the targets of the inner, center, and outer rings were analyzed by single-factor ANOVA, and the results are listed in Table 4.

The droplet deposition densities on the targets of the inner, middle, and outer rings were calculated in different directions (Fig. 11). From the results, the drug loadings on the blades of the inner, center, and outer rings were analyzed.

The standard deviations of the droplet deposition densities on the free, slender, and high spindles were 3.50, 5.25, and 3.38, respectively (inner ring) and 6.83, 6.63, 4.25, respectively (center ring). The droplet deposition densities of the inner and center rings were almost independent of direction. Meanwhile, the droplet deposition densities over the four directions of the outer ring were 10.75, 9.69, and 11.41, respectively, larger than in the inner and center rings. The E and W sides, which were exposed to drug administration from the outer ring, presented a higher density of deposited droplets than the S and N sides. This asymmetry is explained by the smaller spray distance in the E and W directions of the outer ring than in the S and N directions, so the droplet deposition density is more obvious in the E and W directions. However, the spray distances in the inner and middle rings are similar and blocked by layers of blades; accordingly, their droplet deposition densities are smaller and more directionally similar than in

the outer ring. The droplet deposition density gradually increased from the inner to the outer ring (by 52.36% from the inner to center ring, and by 91.27% from the inner to outer ring). The average droplet deposition densities in the middle and outer rings exceeded  $150 \text{ grains}\cdot\text{cm}^{-2}$ . According to this result, applying the medicine to the blades of the middle and outer rings will improve the droplet penetration into regions between the canopy. Although the penetrability of the inner ring was relatively poor, the average droplet deposition density was  $100.60 \text{ grains}\cdot\text{cm}^{-2}$ , exceeding the  $70 \text{ grains}\cdot\text{cm}^{-2}$  stipulated in plant protection operating standards; therefore, it meets the operating requirements of profiling boom sprayer design (GB/T 17997-2008). In summary, the developed profiling boom sprayer provides good droplet penetration from its inner, center, and outer rings, thereby homogenizing the distribution of droplets in the top, middle and bottom layers of the canopy, and achieving the goal of a profiling spray.

## Conclusions

The main conclusions of the study are summarized below.

(1) The overall structure, size, and application parameters of the profiling boom sprayer were determined. The deployment height was 4.0–4.5 m, the spray pressure was 0.6–0.8 MPa, and the spray distance was 1.0–1.5 m.

(2) After averaging over height, the standard deviations of the droplet deposition coverage rates of the free, slender, and high spindles were 4.43, 2.82, and 5.29 respectively, and those of the droplet deposition density were 5.97, 4.98, and 6.15 respectively. All p-values exceeded 0.05, indicating that the outer ring of the profiling boom sprayer evenly distributed the droplets at different heights.

(3) The average droplet deposition densities of the three tree-shaped targets exceeded  $150 \text{ grains}\cdot\text{cm}^{-2}$  in the center and outer rings. The average droplet deposition density in the inner ring was  $100.60 \text{ grains}\cdot\text{cm}^{-2}$ , and the droplet deposition coverage rates of the free, slender, and high spindles were 37.41%, 36.69%, and 35.47%, respectively.

(4) The developed profiling boom sprayer improves the inherent serious drift problem of the air blower sprayer, and can inspire the research and development of orchard plant protection machinery. The prototype design parameters may provide a basis for subsequent improvement of the profiling boom sprayer.

## Declarations

### Acknowledgments

This work is supported by the earmarked fund for Agriculture Research System of China (CARS-27), the earmarked fund for Hebei Fruit Innovation Team of Modern Agro-industry Technology Research System (HBCT2018100205).

## Authors' Contributions

**Conceptualization:** Peng Huo; Jianping Li **Data acquisition:** Peng Huo; Jianping Li **Data analysis:** Peng Huo **Design of methodology:** Peng Huo **Software development:** Peng Huo **Writing and editing:** Peng Huo; Jianping Li

## References

1. Bahlol, H. Y., Chandel, A. K., Hoheisel, G. A., & Khot, L. R. (2020). The smart spray analytical system: Developing understanding of output air-assist and spray patterns from orchard sprayers. *Crop. Prot.*, 127, 104977..
2. Baldoin, C., De Zanche, C., & Bondesan, D. (2008). Field testing of a prototype recycling sprayer in a vineyard: Spray distribution and loss. *Agricultural Engineering International: CIGR Journal*. Vol. X . May.
3. Balsari, P., Gil, E., Marucco, P., van de Zande, J. C., Nuyttens, D., Herbst, A., & Gallart, M. (2017). Field-crop-sprayer potential drift measured using test bench: Effects of boom height and nozzle type. *Biosyst. Eng.*, 154, 3-13.
4. Berk, P., Stajanko, D., Belsak, A., & Hocevar, M. (2020). Digital evaluation of leaf area of an individual tree canopy in the apple orchard using the LIDAR measurement system. *Comput. Electron. Agric.*, 169, 105158.
5. Chi, M., Guanglin, L., & Xiaodong, L. (2019). Development of multi-orientation automatic spraying device for citrus orchards in hilly and mountainous areas. *Trans. Chin. Soc. Agric. Eng.*,35(3), 31-41.
6. Duga, A. T., Delele, M. A., Ruysen, K., Dekeyser, D., Nuyttens, D., Bylemans, D., ... & Verboven, P. (2017). Development and validation of a 3D CFD model of drift and its application to air-assisted orchard sprayers. *Biosyst. Eng.*, 154, 62-75.
7. Duga, A. T., Ruysen, K., Dekeyser, D., Nuyttens, D., Bylemans, D., Nicolai, B. M., & Verboven, P. (2015). Spray deposition profiles in pome fruit trees: Effects of sprayer design, training system and tree canopy characteristics. *Crop. Prot.*, 67, 200-213.
8. Gao, G., Xiao, K., & Li, J. (2018). Precision Spraying Model Based on Kinect Sensor for Orchard Applications. *Appl. Eng. Agric.*, 34(2), 291-298.
9. Garcerá, C., Doruchowski, G., & Chueca, P. (2020). Harmonization of plant protection products dose expression and dose adjustment for high growing 3D crops: A review. *Crop. Prot.*, 105417.
10. GB/T 17997-2008, Evaluating regulations for the operation and spraying quality of sprayers in the field. China.
11. Gil, E., Balsari, P., Gallart, M., Llorens, J., Marucco, P., Andersen, P. G., ... & Llop, J. (2014). Determination of drift potential of different flat fan nozzles on a boom sprayer using a test bench. *Crop. Prot.*, 56, 58-68.
12. Giles, D. K., Delwiche, M. J., & Dodd, R. B. (1989). Sprayer control by sensing orchard crop characteristics: orchard architecture and spray liquid savings. *Journal of Agricultural Engineering*

Research, 43, 271-289.

13. Herbst, A., Osteroth, H. J., & Stendel, H. (2018). A novel method for testing automatic systems for controlling the spray boom height. *Biosyst. Eng.*, 174, 115-125.
14. Hołownicki, R., Doruchowski, G., Świechowski, W., Godyń, A., & Konopacki, P. J. (2017). Variable air assistance system for orchard sprayers; concept, design and preliminary testing. *Biosyst. Eng.*, 163, 134-149.
15. Jamar, L., Mostade, O., Huyghebaert, B., Pigeon, O., & Lateur, M. (2010). Comparative performance of recycling tunnel and conventional sprayers using standard and drift-mitigating nozzles in dwarf apple orchards. *Crop. Prot.*, 29(6), 561-566.
16. Kira, O., Dubowski, Y., & Linker, R. (2018). In-situ open path FTIR measurements of the vertical profile of spray drift from air-assisted sprayers. *Biosyst. Eng.*, 169, 32-41.
17. Landers, A., & Muise, B. (2010). The development of an automatic precision canopy sprayer for fruit crops. *Aspects of Applied Biology*, (99), 29-34.
18. Lin, J., Ma, J., Liu, K., Huang, X., Xiao, L., Ahmed, S., ... & Qiu, B. (2021). Development and test of an autonomous air-assisted sprayer based on single hanging track for solar greenhouse. *Crop. Prot.*, 142, 105502.
19. Ma, L., Xu, Y., Zheng, J., & Dai, X. (2020). Ecodesign method of intelligent boom sprayer based on Preferable Brownfield Process. *J. Clean. Prod.*, 268, 122206.
20. Nan, Y., Zhang, H., Zheng, J., Jiao, X., Xu, Y., & Wang, G. (2019). Ultrasonic quantification test of plant canopy density based on cylindrical surface model. *Trans. Chin. Soc. Agric. Mach.*, 50(1).
21. NY/T 992-2006, The operation quality for air-assisted orchard sprayer. China.
22. Peteinatos, G. G., Kollenda, B., Wang, P., & Gerhards, R. (2019). A new logarithmic sprayer for dose-response studies in the field. *Comput. Electron. Agric.*, 157, 166-172.
23. Salcedo, R., Zhu, H., Zhang, Z., Wei, Z., Chen, L., Ozkan, E., & Falchieri, D. (2020). Foliar deposition and coverage on young apple trees with PWM-controlled spray systems. *Comput. Electron. Agric.*, 178, 105794.
24. Torrent, X., Gregorio, E., Rosell-Polo, J. R., Arnó, J., Peris, M., van de Zande, J. C., & Planas, S. (2020). Determination of spray drift and buffer zones in 3D crops using the ISO standard and new LiDAR methodologies. *Sci. Total. Environ.*, 714, 136666.
25. Wang, Y., Li, W., Xu, X., Qiu, C., Wu, T., Wei, Q., ... & Han, Z. (2019). Progress of apple rootstock breeding and its use. *Hortic. Plant. J.*, 5(5), 183-191.

## Tables

**Table 1.** Key application parameters of the profiling boom sprayer

Parameters	Value
Average crown size $a$ (m)	0.8–1.2
Plant spacing $b$ (m)	1.1–1.5
Row spacing $c$ (m)	3.5–4.0
Height of mature tree $h$ (m)	3.5– 4.0
Nozzle atomization angle $\varphi$ (°)	60, 80, 110
Nozzle pressure $A$ (MPa)	0.6–0.8
Spray distance $B$ (m)	1.0–1.5
Nozzle spacing $C$ (m)	0.3–0.4
Spread Height $H$ (m)	4.0–4.5

Table 2. Droplet deposition coverage rates (single-factor analysis of variance results) on the targets at different heights in a given direction.

Tree shape	Direction	Square sum	Freedom	Mean square	F value	p value
Free spindle	East	56.00	2	28.00	1.24	0.32
	West	9.06	2	4.53	0.24	0.79
	South	7.01	2	3.51	0.17	0.84
	North	39.09	2	19.55	1.53	0.26
Slender spindle	East	24.70	2	12.35	0.64	0.54
	West	30.67	2	15.33	0.67	0.53
	South	6.37	2	3.18	0.22	0.80
	North	54.14	2	27.07	1.04	0.38
High spindle	East	41.33	2	20.66	0.91	0.42
	West	11.98	2	5.99	0.28	0.76
	South	45.08	2	22.54	0.53	0.59
	North	39.09	2	19.55	0.51	0.61

Table 3. Droplet deposition densities (single-factor ANOVA results) on the targets at different heights in the same direction.

Tree shape	Direction	Square sum	Freedom	Mean square	F value	p value
Free spindle	East	76.16	2	38.08	0.88	0.43
	West	5.63	2	2.81	0.03	0.96
	South	58.55	2	29.27	0.53	0.59
	North	15.27	2	7.64	0.27	0.76
Slender spindle	East	29.89	2	14.95	0.46	0.64
	West	45.09	2	22.55	0.51	0.60
	South	7.63	2	3.82	0.13	0.87
	North	25.32	2	12.66	0.64	0.54
High spindle	East	1.86	2	0.93	0.01	0.99
	West	120.98	2	60.49	0.52	0.60
	South	929.13	2	464.56	2.91	0.08
	North	28.47	2	14.24	0.08	0.92

**Table 4.** Droplet deposition densities (single-factor ANOVA results) on the targets of the inner center and outer rings in different directions

Tree shape	Area	Square sum	Freedom	Mean square	F value	p value
Free spindle	Inner ring	57.05	3	19.02	1.60	0.22
	Center ring	11.37	3	3.79	0.07	0.97
	Outer ring	1123.85	3	374.61	4.54	0.01
Slender spindle	Inner ring	87.98	3	29.328	1.02	0.40
	Center ring	120.00	3	40.00	0.85	0.48
	Outer ring	591.97	3	197.32	3.22	0.04
High spindle	Inner ring	59.93	3	19.97	1.86	0.16
	Center ring	19.36	3	6.45	0.31	0.81
	Outer ring	1497.24	3	499.08	6.11	<0.01

## Figures

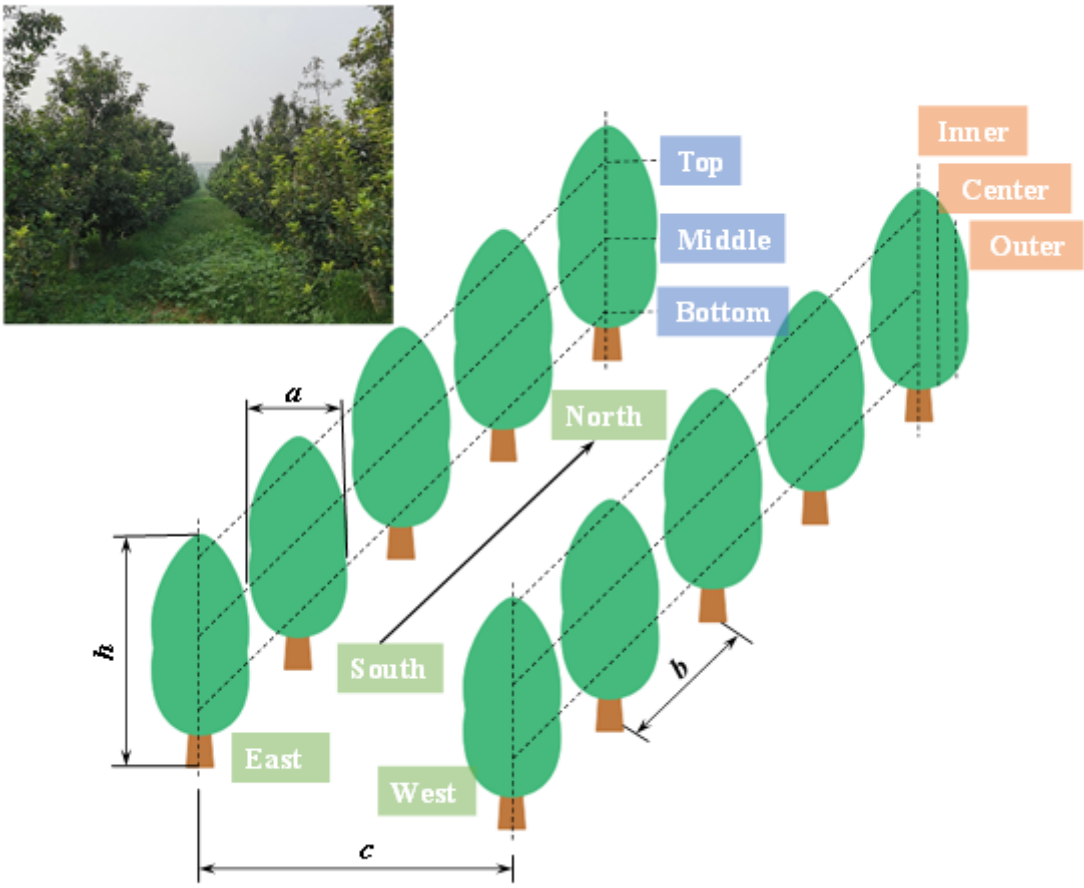


Figure 1

Modern dwarf rootstock and densely planted apple orchard.

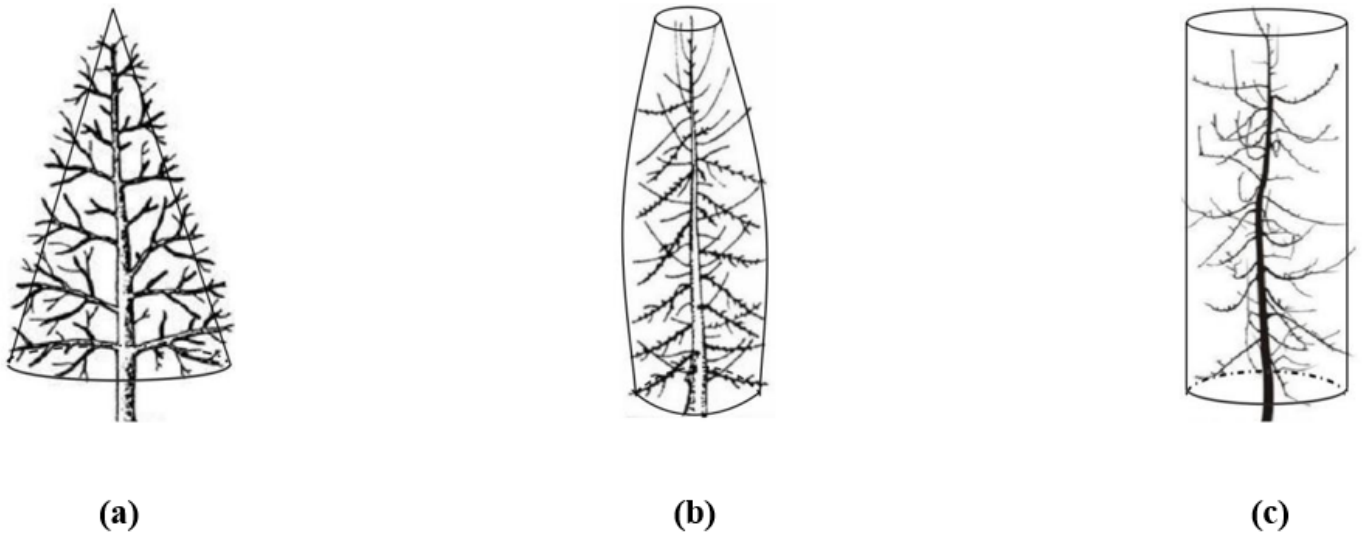
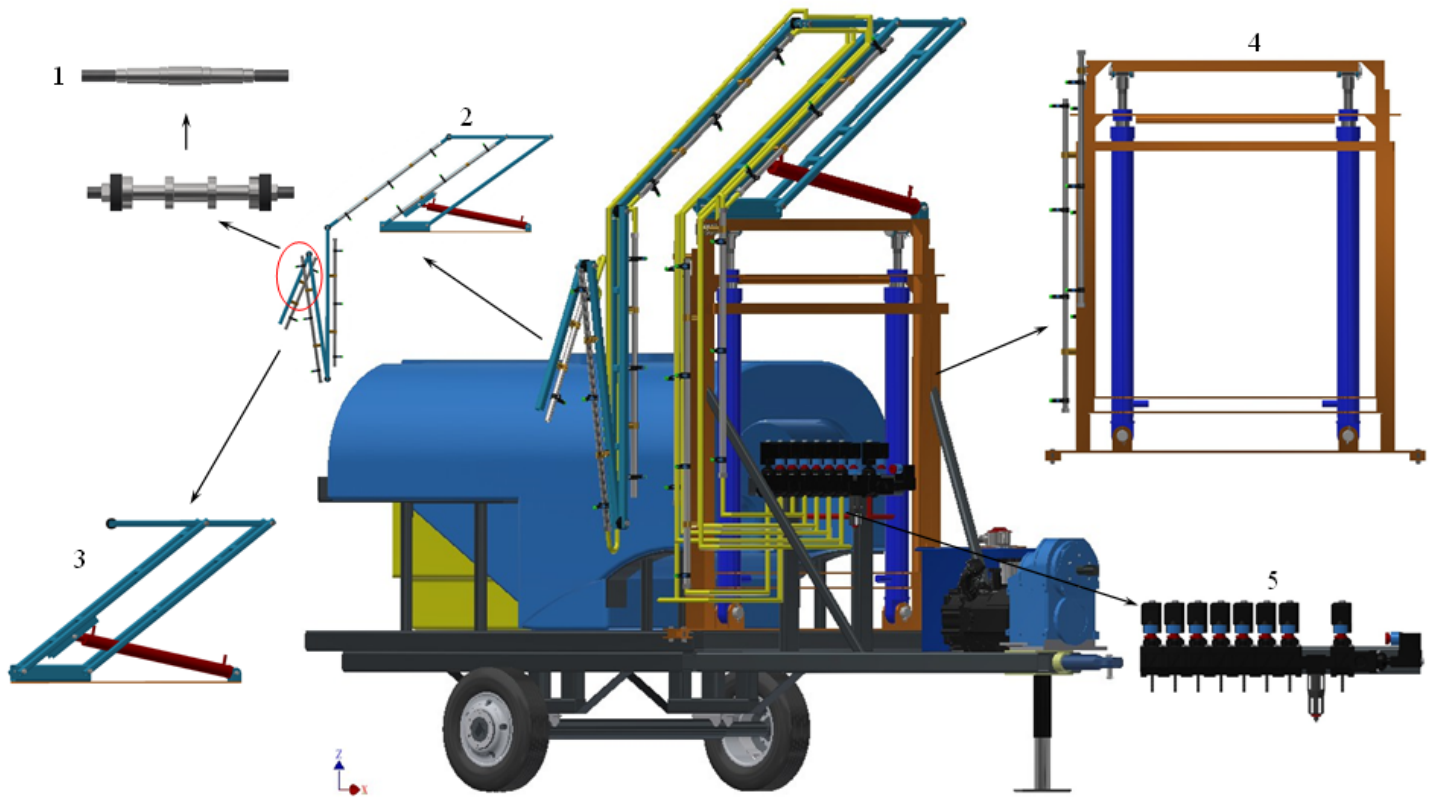


Figure 2

Main tree shapes of dwarf rootstock close-planting orchards: (a) free spindle, (b) slender spindle, and (c) high spindle.



**Figure 4**

Structure of the profiling boom sprayer. (1) Joint shaft; (2) Boom group; (3) Folding–unfolding mechanism; (4) Lifting mechanism; (5) Solenoid valve group.

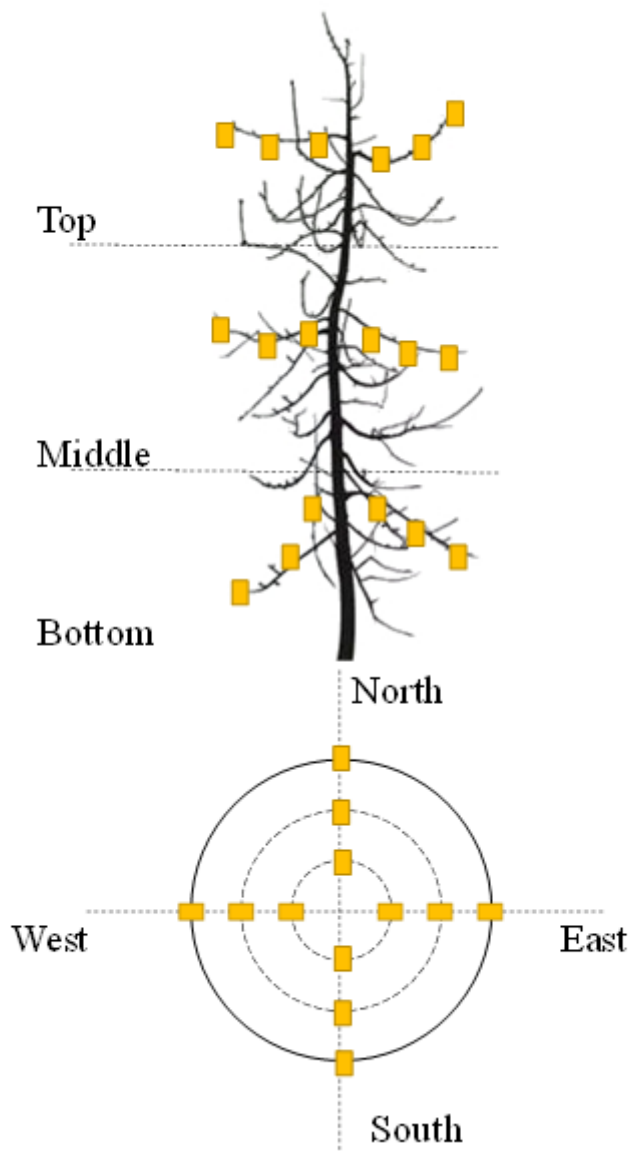


**Figure 5**

Layout of water-sensitive papers at the test site.

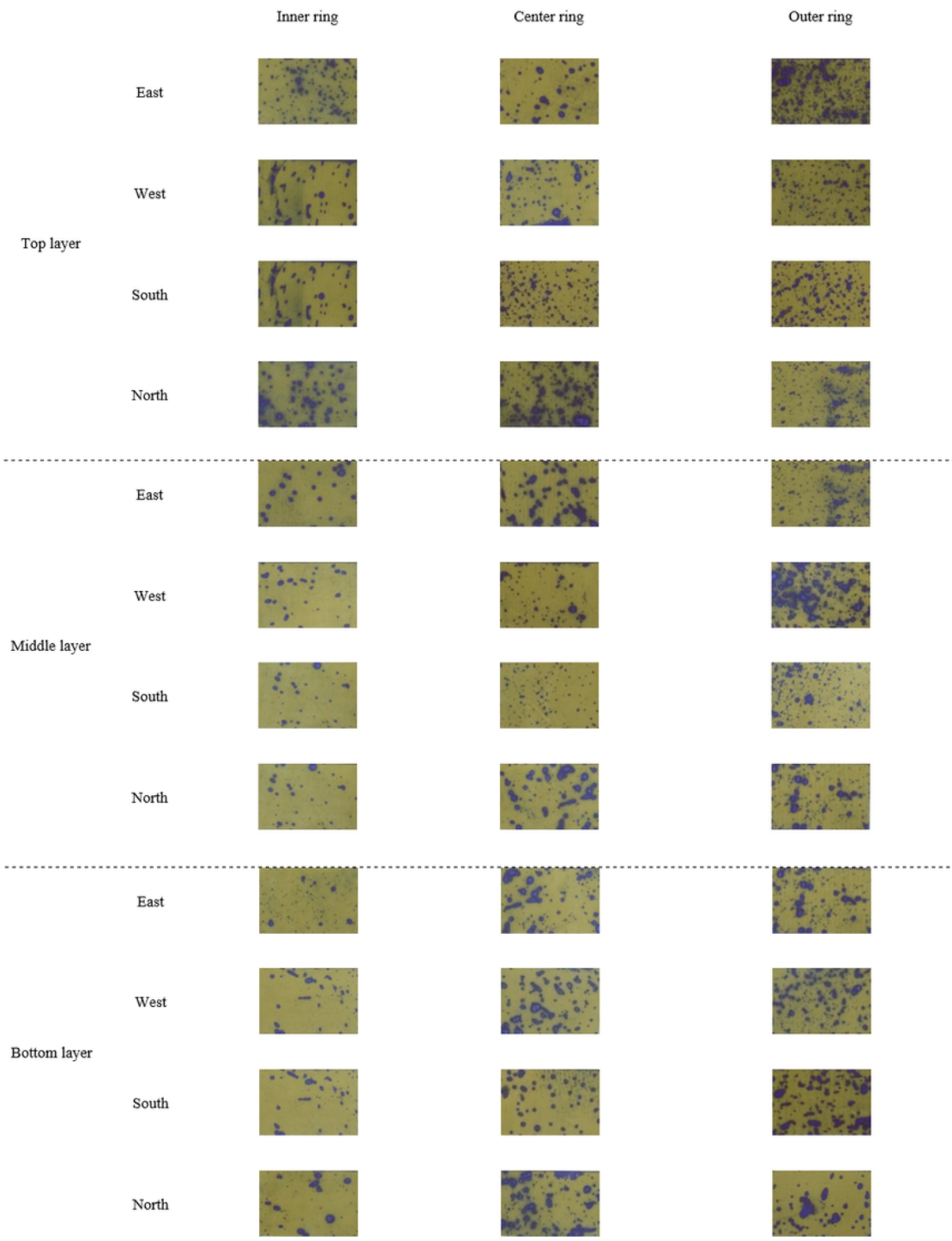


**Figure 6**

Example of droplet distribution on water-sensitive paper at one test target.

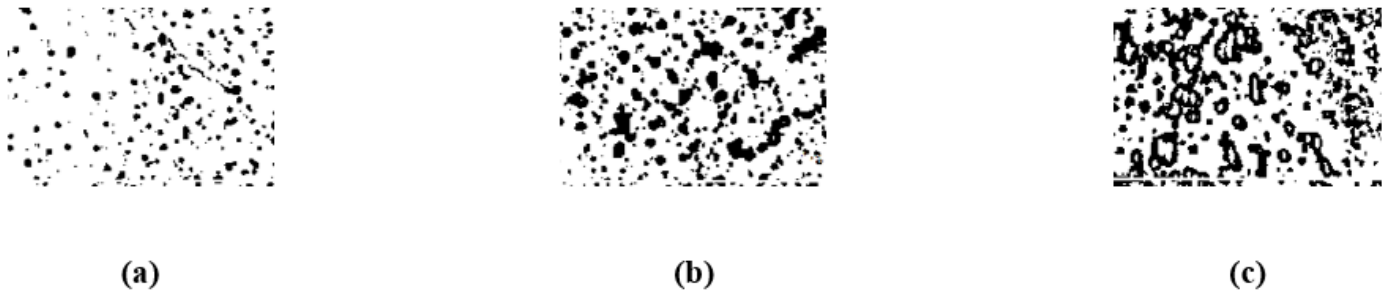


**Figure 7**

Water-sensitive paper in figure 6 after processing: (a) Inner ring, (b) Center ring, and (c) Outer ring.

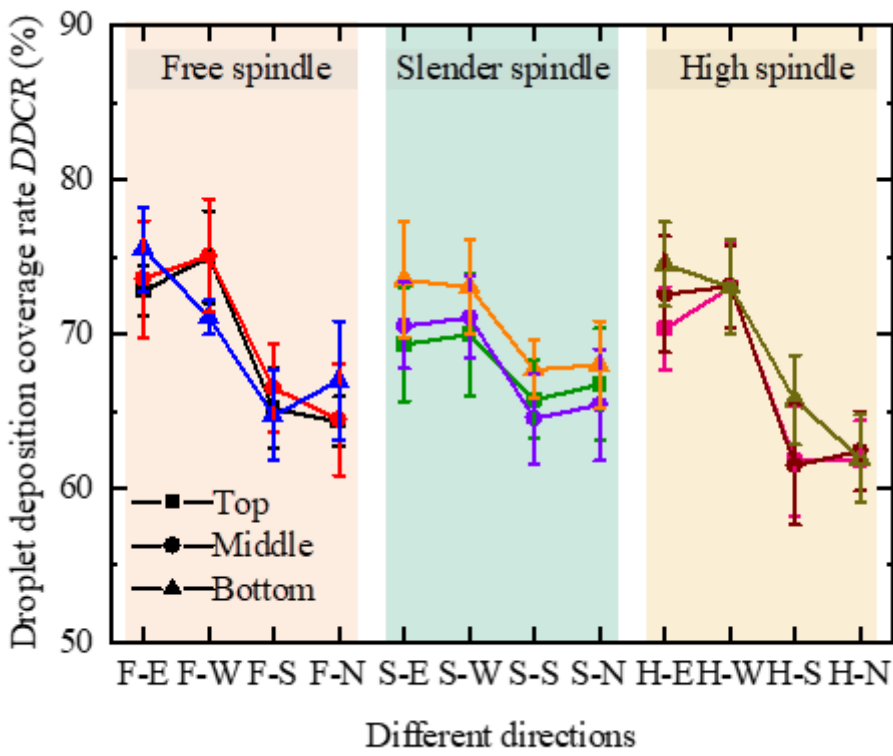


**Figure 8**

Droplet deposition coverage rates of the targets of the outer ring.

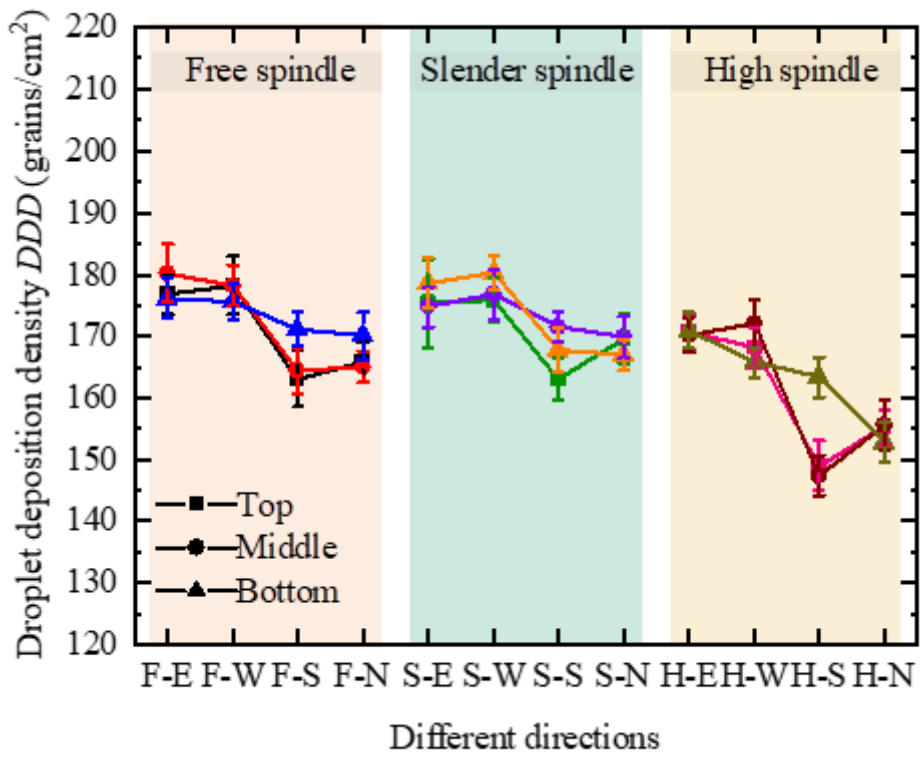


Figure 9

Droplet deposition densities on the targets of the outer ring.

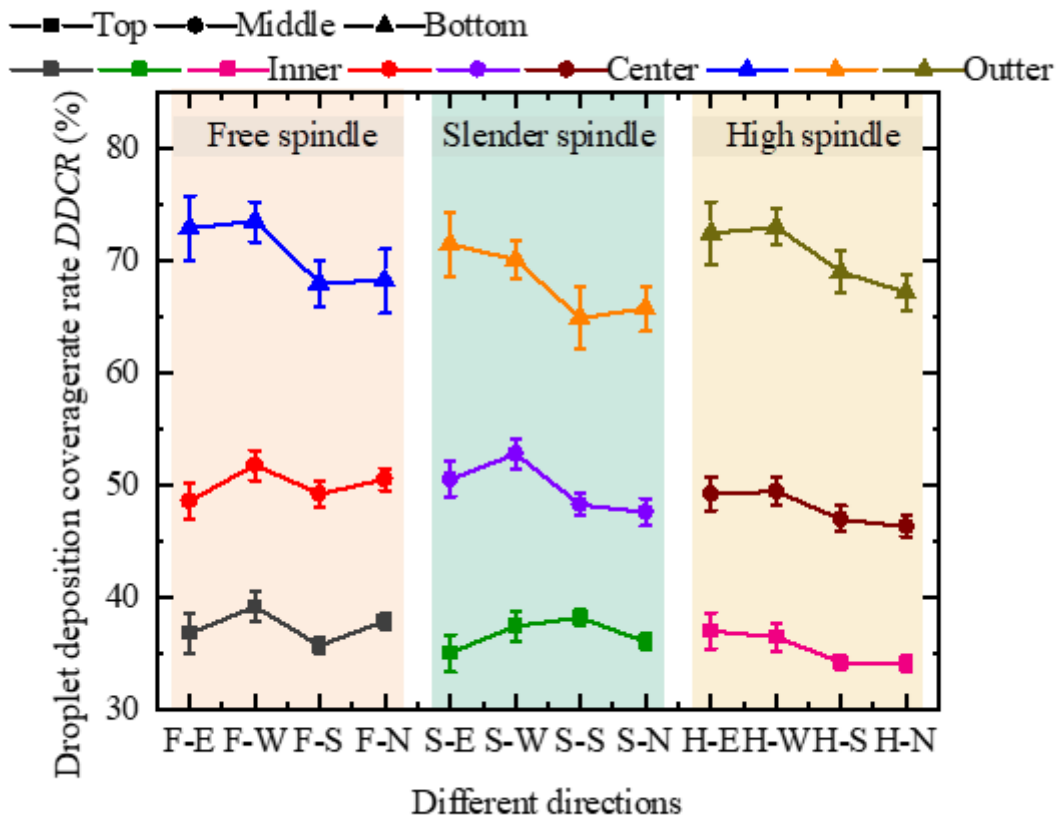


Figure 10

Droplet deposition coverage rates on the targets of the inner, center, and outer rings.

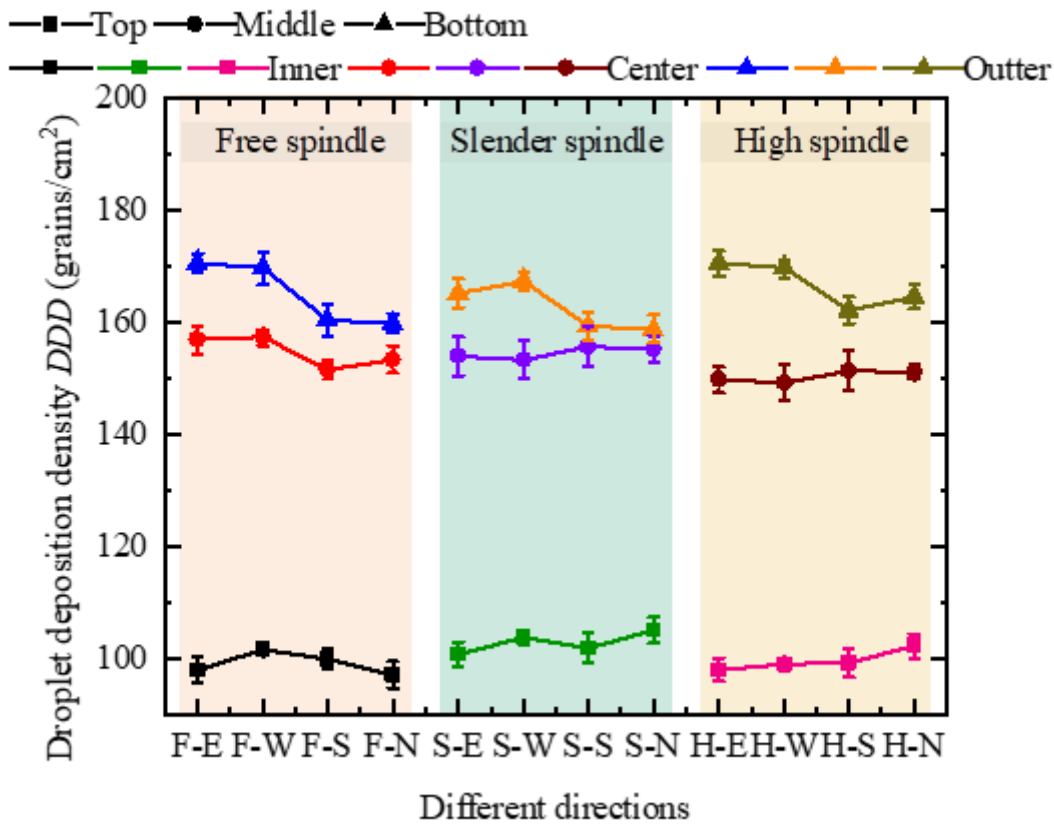


Figure 11

Droplet deposition densities on the targets of the inner, center, and outer rings.